
Article:
Tomeh, M.A. and Zhao, X. orcid.org/0000-0002-4620-2893 (2020) Recent advances in microfluidics for the preparation of drug and gene delivery systems. Molecular Pharmaceutics, 17 (12). pp. 4421-4434. ISSN 1543-8384

https://doi.org/10.1021/acs.molpharmaceut.0c00913

Recent advances in microfluidics for preparation of drug and gene delivery systems

Mhd Anas Tomeh[1] and Xiubo Zhao [1,2, *]

[1] Department of Chemical and Biological Engineering, University of Sheffield, Sheffield S1 3JD, UK

[2] School of Pharmacy, Changzhou University, Changzhou 213164, China

* Correspondence: xiubo.zhao@sheffield.ac.uk; Tel.: +44-(0)-0114-222-8256

Abstract

Drug delivery systems (DDSs) have a great potential for improving the treatment of several diseases, especially microbial infections and cancers. However, the formulation procedures of DDSs remain challenging especially at the nanoscale. Reducing batch-to-batch variation and enhancing production rate are some of the essential requirements for accelerating the translation of DDSs from small scale to industrial level. Microfluidic technologies have emerged as an alternative to the conventional bench methods to address these issues. By providing a precise control over the fluid flows and rapid mixing, microfluidic systems can be used to fabricate and engineer different types of DDSs with specific properties for efficient delivery of a wide range of drugs and genetic materials. This review discusses the principles of controlled rapid mixing that have been employed in different microfluidic strategies for producing DDSs. Moreover, the impact of the microfluidic device design and parameters on the type and properties of DDS formulations were assessed and recent applications in drug and gene delivery were also considered.

Keywords: Microfluidics, rapid mixing, tunable properties, nanomedicine, drug delivery systems

TOC Fig

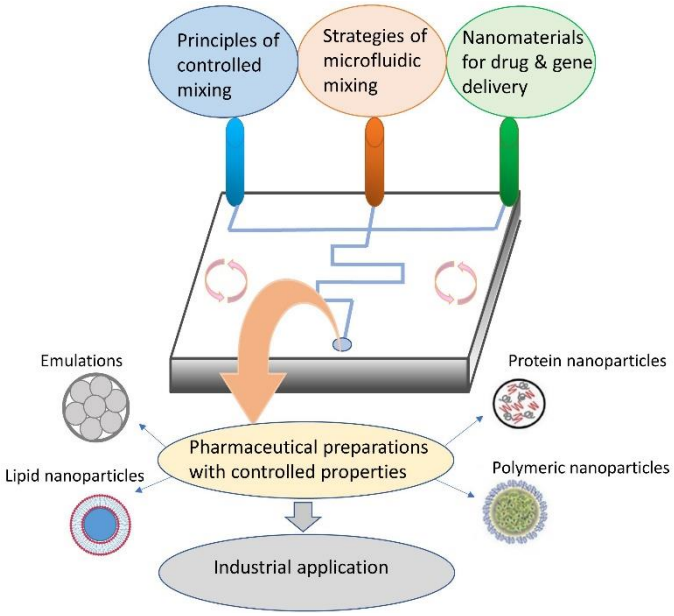

1 Introduction

In the past decade, enormous advancement in the field of nanotechnology was achieved to produce nanoformulations for drug and gene delivery [1-3]. Employing this nanotechnological advancement in nanomedicine opened doors for improving some of the most challenging therapies such as cancer treatments. Designing nanoformulations with controlled size and features offers many advantages including enhanced drug encapsulation, controlled release of the payloads, improved targetability and enhanced cellular uptake [4, 5]. In addition, encapsulating the active pharmaceutical ingredients (APIs) such as anticancer drugs within nanocarriers can enhance *in vivo* stability, and increase their blood circulation time [6]. In spite of all these advantages, only few nanoformulations have made to clinical trials such as Doxil®, Caelyx®, Myocet® and Abraxane® due to technical challenges in formulating many pharmaceutical materials [7]. Fabricating pharmaceutical nanomaterials can be achieved using top-down or bottom-up approaches. In general, top-down approach is not suitable for processing many (APIs) due to high shear forces involved in the mechanical milling [8-10]. In the bottom-up approach, the formation of nanostructures is performed by converting the molecular matter dissolved in liquid to particulate forms. Based on the nature and composition of the fabricated drug delivery systems (DDSs), the nanostructures are formed by self-assembly, emulsification or precipitation [11-17]. One of the main considerations in formulating different types of polymers or APIs, is to maintain the dimensions of the designed particles within a range of 100-300 nm which is desirable for pharmaceutical applications [18]. A frequently used technique to prepare DDSs with controlled size is mixing amphiphile (e.g., liposomes or micelles) solutions with antisolvent or polyelectrolyte solutions (e.g., cationic polymers or nucleic acids) [19, 20]. DDSs will precipitate or self-assemble as a result of the hydrophobic or electrostatic interactions. Despite the great potential that nano-sized DDSs possess *in vitro*, they demonstrated slow translation to clinical applications. This limitation is due to challenges such as production of large quantities and reproducibility of prepared nanostructures of the DDSs [21]. Many studies have shed more light on the mixing kinetics in order to control the properties of the fabricated DDSs such as size, polydispersity and the API encapsulation efficiency [22-25]. Among several mixing techniques, microfluidic systems have received the most attention due to their ability to control mixing, low running cost and amenability to modifications [26]. In comparison to bulk production methods, microfluidic synthesis/formulation of single or multicomponent nanoparticles (NPs) has shown higher controllability and reproducibility [27-29]. The newly developed microfluidic devices provided a platform for preparing different formulations of DDSs including multiple emulations [30, 31], protein-based nanoparticles [32, 33], liposomes [34, 35] and polymeric nanoparticles [36]. There are several reported microfluidic devices that have implemented the principles of rapid and controlled mixing for preparing a myriad of DDSs. In addition, the microfluidic platform has helped overcoming some obstacles in DDSs fabrication such as purification, functionalization and large-scale production [37, 38]. This review presents the recent developments in microfluidics and its application in drug and gene delivery. In the first part, the basic principles of controlled mixing and flow regimes are summarized to provide a theoretical background for rational design of microfluidic devices. Subsequently, the most common microfluidic design strategies are discussed with an emphasis on recent applications in pharmaceutical preparations. The properties of the DDSs that can be controlled by the microfluidics were discussed followed by a summary of different types of the DDSs prepared by the microfluidics for drug and gene delivery applications. The challenges for the industrial application of microfluidics for DDS fabrication were also included.

2 Principles of mixing under controlled conditions

2.1 Rapid nanoprecipitation

Fast precipitation is a widely used process in the pharmaceutical field as a bottom-up approach to prepare small molecule drug nanoparticles or to formulate multicomponent nanocarriers for drug delivery. The basis of nanoparticle formation has been explained by the classical crystallization theory [9, 39]. In single phase system, rapid precipitation occurs when a highly supersaturated condition is reached as a result of sudden change in precipitation dependant conditions such as concentration or temperature. The precipitation process begins with nucleation when solid seeds emerge from the liquid phase to achieve thermodynamic stability. This phase separation is governed by the force generated by the reduction from the high Gibbs free energy (ΔG) of supersaturation state to low ΔG which is more favourable thermodynamically. The nucleation rate (B) can be calculated using this energy difference according to Equation (1) [40]:

$$B = A\ exp\left(\frac{-\Delta G}{kT}\right) \quad (1)$$

Where *A* is a constant, *k* is Boltzmann's constant, *T* is the absolute temperature and *ΔG* is the Gibbs free energy of nucleation. Assuming the outcome of nucleation is spherical particles with critical radius (r_c), the nucleation rate can also be given by Equation (2) [41]:

$$B = A\ exp\left(\frac{-16\pi\gamma^3 v^2}{3k^3T^3[ln\ (s_r)]^2}\right) \quad (2)$$

Where *A* is a constant, *γ* is the surface tension, *v* is the molar volume, *k* is Boltzmann's constant, *T* is the absolute temperature and S_r is the supersaturation ratio. Both equations 1&2 demonstrate that nucleation and particle growth are govern by supersaturation, as well as temperature [39, 41]. Therefore, the mechanism by which supersaturation is achieved can control particle formation and growth at a given temperature. The nanoprecipitation of particles requires creating the supersaturation condition by rapid mixing of two or more miscible liquids. When one solution containing the solute (drug or polymer) meets an anti-solvent in the mixer channels, nucleation and particle growth of the solute are triggered (Figure 1). Optimizing mixing parameters between solution and anti-solvent such as reducing mixing time (t_{mix}), selecting the mixer geometry and flow regime can cause the least variation in supersaturation conditions and thus the least variation in particle properties. However, there are several other parameters that must be considered to modify the properties of the nanoparticles produced by nanoprecipitation. These involve: (1) the hydrophobicity of the drug or polymer, (2) the selection of the solvent and anti-solvent, (3) addition of stabilizers to minimize agglomeration [39, 41, 42].

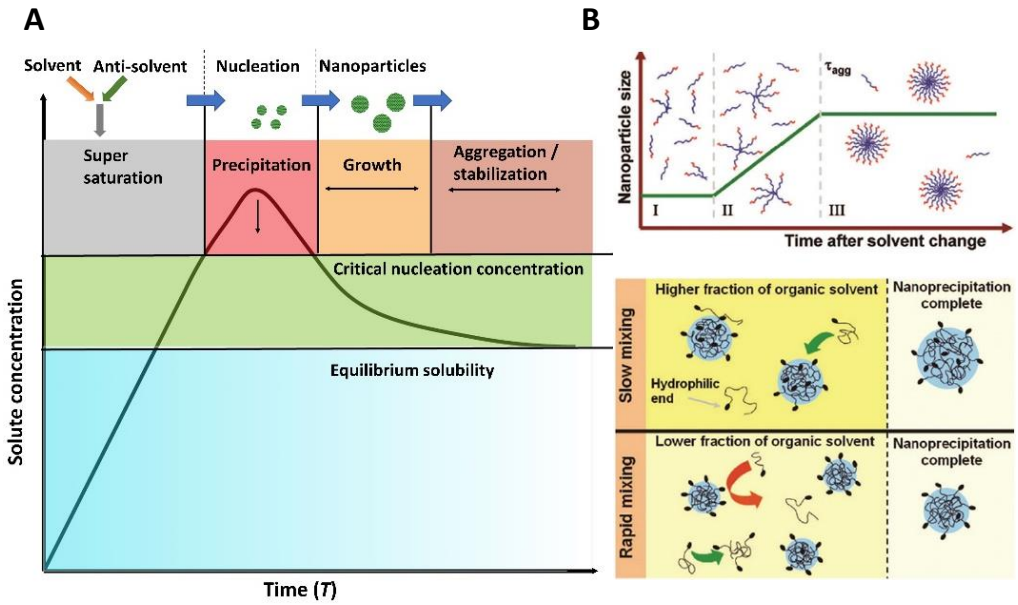

Figure 1. A) Schematic representation of solute concentration trend during the nanoprecipitation and nanoparticle formation steps. **B)** The staged assembly process of block copolymers to form nanoparticles and the effect of rapid mixing on the properties of the produced nanoparticles. Reprinted from [43] with the permission from ACS Publications.

2.2 Flow regimes and Reynolds number

The production of nanoformulations using nanoprecipitation of small molecules, controlled crosslinking of polymers, or structural transformations of proteins requires rapid mixing [32, 44]. In nanoprecipitation, mixing in small timescale (milliseconds to microseconds) can create uniform local high supersaturation leading to nanoprecipitation of any molecule above the saturation level regardless of its nature [41, 45]. This mechanism has been exploited to formulate many hydrophobic drugs in pharmaceutical industry [43]. The interaction of two fluids can be classified into two regimes: laminar and turbulent. Laminar flow occurs when the mixed fluids flow in parallel layers or paths without forming perpendicular or opposite currents to the main flow. On the other hand, turbulent flow takes place when the fluids undergo irregular fluctuation leading to continual mixing in both magnitude and direction [9]. The type of flow within the mixer chamber is governed by viscous forces and inertial forces (resistance and driving forces) which is measured by Reynolds number (Re) in Equation (3)[46]:

$$Re = \frac{\rho u D_h}{\mu} = \frac{u D_h}{v} \tag{3}$$

where ρ is fluid density; μ is dynamic viscosity; v is the fluid kinematic viscosity; u is a mean fluid velocity and D_h is a hydraulic diameter of the channel of the mixer. The design and geometry of the mixing channels is corelated to its hydraulic diameter, and is given by Equation (4)[46]:

$$D_h = \frac{4A}{P_{wet}} \tag{4}$$

where A is the channel cross-sectional area and P_{wet} are wetted perimeter. Turbulent flows regime dominates at relatively high Reynolds number (Re >4000) and the range between Re=2100 and 4000 is unsteady flow and its complexity is highly dependent on the mixer geometry. As a result of the

random motion of fluid streams in multiple directions in time and space, the mass transfer by advection occurs in all spatial directions in the turbulent flow regime [47]. On the contrary, laminar flow is associated with low Reynolds number (Re <2100) and the advective mass transport can only happen in the direction of the main flow [46]. The majority of microfluidic devices use low Re and which corresponds to laminar flow. In this regime, mixing relies on passive diffusion and advection. The molecular movement form high concentration to a lower concentration domain is defined as Diffusion-based mass transfer and can be calculated using Fick's laws Equation (5) [48]:

$$J = -D\frac{d\varphi}{dx} \tag{5}$$

Where φ is the concentration; D is the diffusion coefficient and x represent the spatial coordinates. The diffusion coefficient is given by Stokes–Einstein Equation (6)[49]:

$$D = \frac{kT}{6\pi\mu r} \tag{6}$$

Where k is Boltzmann's constant; T is the absolute temperature; r is the particle radius and μ is the fluid viscosity. For small molecules dissolved in water at constant ambient temperature, D can be considered as 10^{-10} m^2s^{-1} [50]. Diffusion does not happen at once; but it is a gradual process which takes into account the time factor t and fluids are non-linearly diffuse over distance x. Therefore one-dimensional diffusion process follow the Equation (7) [51]:

$$x^2 = 2Dt \tag{7}$$

Where x^2 is the mean square distance diffused in time t. Since many microfluidic systems use laminar flow, diffusion has become the main consideration for manipulating rapid mixing and controlling particle production. Based on Equations (5 & 6), modifying the diffusion process can be done by altering the viscosity (changing the solvent quality) by changing one or more of the mixed solvents. Moreover, reducing the diffusion distance x in the microchannels of the mixer results in shorting the time required for mixing (Equation 7) [52]. Therefore, these factors have provided guidelines for the design of microfluidic device and optimization of particle production by rapid mixing.

3 Strategies and mechanisms for controlling the formation of DDSs

Polymeric molecules such as amphiphilic block copolymers, lipids and polyelectrolytes (e.g., oligonucleotides) can precipitate or self-assemble into nanostructures when changing the solvent quality by mixing. For example, rapid mixing of the solvent (polymeric solution) with antisolvent affects the size and size distribution of the formed particles [53]. As discussed earlier, mixing time scale t_{mix} is a key factor in rapid mixing. Another essential factor is nucleation time t_{agg}, which is the timescale required for seeds or chains of the material to aggregate and grow (Figure 1). Determining t_{agg} is quite difficult because it depends on the molecular weight of the building block and ranges from 10 to 100 ms [1]. Large and polydisperse particles are produced when aggregation is favoured due to lack of stabilization of the formed nanoparticles in the heterogeneous mixing environment. On the other hand, the homogeneous solvent environment (complete solvent change) stabilizes the hydrophilic part of the amphiphilic molecules leading to small size distribution of the formed particles. This state occurs only when $t_{mix} < t_{agg}$ and the stabilization of the nanoparticles will be favoured [54]. Unlike conventional mixing methods, which require a timescale of seconds, microfluidic devices allow for

controllable rapid mixing within milliseconds [43, 55]. For example, lipid nanoparticles (LNPs) have been prepared by organic solvent injection method using several microfluidic devices. At the liquid-liquid interface, the polarity of the solvent increases rapidly because of molecular diffusion leading to the formation of LNPs [34]. Studies have shown that manipulating dimensions and design of microfluidic device affects the molecular diffusion and NLP properties [56, 57]. Moreover, reducing the mixing time in the micromixer has shown a significant impact on the particle formation and growth kinetics [58]. Different microfluidics systems have different geometric designs which can change the particle formation mechanism.

3.1 T-mixer and co-flowing junction

T-junction is one of the earliest and simplest geometric designs of microfluidic devices. Organic solvent meets the aqueous phase in a perpendicular manner and in some designs the two inlets merge in a sharp angle (< 90 °) to form a Y-like shape (Figure 2A) [26, 59]. By using co-flowing channels, droplets can be formed as water-in-oil (W/O), oil-in-water (O/W) or double oil-in-water-in-oil (O/W/O) [60]. In Y-shaped devices, the mixing occurs at the aqueous/solvent interface in the main channel surface and the key factor which affects mixing (t_{mix}) is the diffusion rate. t_{mix} of fluids tends to be long at relatively low *Re,* because the flow regime which is dominating is laminar. Therefore, the geometric design of these devices have been modified and higher flow rates were applied to generate perturbations that can improve mixing efficiency [61]. As discussed before, the phase change in nanoprecipitation is triggered by exceeding supersaturation threshold. This can be achieved in a T-mixer at crucial mixing conditions such as short t_{mix} to allow for homogeneous nucleation. One of the efficient mechanisms to reduce t_{mix} is enhancing the turbulence to increase the fluid interface, which can be achieved by rapid mixing at high flow rate [62]. T-mixer design can provide a wide range of mixing from the laminar to the turbulent regime (e.g. Schikarski et *al*, investigated the *Re* from 100 to 4000) [63], which can be utilized for preparation of different nanoformulations. Figure 2B shows an accurate simulation of small molecule precipitation in a rectangular T-mixer [64]. To enhance the mixing efficiency between two miscible liquids within the microchannels, Günther et *al.* [65] proposed a segmented gas-liquid flow strategy [65, 66]. This strategy increases the advection mixing of the two liquid streams in a straight microchannel by introducing a gas phase which generates a segmented gas-liquid flow. The separation of the mixed liquids and gas streams reduces the mixing time and allows for shortening the mixing length [65, 66].

3.2 Hydrodynamic flow focusing

Hydrodynamic flow focusing (HFF) mixing is one of the most applicable technique for continuous production of different types of DDSs such as polymeric nanoparticles, liposomes and nano-emulations [3, 67, 68]. The principle of HFF mixing relies on a stream of dispersed phase, containing lipids or polymeric materials, flows through a central micro channel to encounter streams of the continuous phase which is known as sheath streams (Figure 2C) [69]. Mixing the two streams takes place at restricted space which allows for droplet formation at controlled laminar flow conditions. This liquid-liquid interface can generate LNPs and polymeric nanoparticles [70]. The mixing time can be tuned in HFF by changing the diameter of the central channel which modify the width of the focused stream [71].

There are different HFF geometric designs that have been developed for controlling the properties of the produced nanoformulation. Xu et *al*. [12] reported a simple HFF design consists of coaxial glass capillary-based microfluidic channel and a nozzle inside a round capillary (Figure 2C). The organic dispersed phase containing PLGA was steadily jetted from the nozzle into a larger capillary which

contains the continuous aqueous phase leading to small-droplet emulations. This device allows for burst nucleation and fast ripening of the PLGA nanoparticles after the molecular diffusion of the organic solvent. Three-dimensional (3D) HFF (Figure 2D) for liposome synthesis was developed by Hood et *al.* [72]. Unlike 2D HFF devices with horizontal channel surfaces in the interfacial mixing region, 3D design removed these surfaces. This approach reduces the migration distance of the organic stream and accelerate lipid convection to the mixing interface [72]. 2D and 3D HFF techniques have been widley applied in pharmaceutical industy to produce several formulations (Table 1). The mixing time required for complete mixing in HFF devices depends on the microchannel design. For example, the complete diffution of two fluids in two HFF designs (single & double hydrodynamic focsing) are 3.33 and 1.29 ms, respectively [3].

3.3 Multi-inlet vortex mixers

Multi-inlet vortex mixer (MIVM) have been designed to facilitate large scale production of polymeric particle by rapid nanoprecipitation [73]. In this system, four streams of fluids (two organic solvents & two aqueous solutions) enter the mixer from different inlets allowing for highly efficient mixing of all components in the solvent mixture (Figure 2E&F). A high supersaturation level can built up over a very short time leading to rapid nanoprecipitation and formation of nanoparticles with small size distributions [73]. Compare to T-mixers, MIVM has shown more product conversion efficiency and higher product yield [45]. However, requiring identical or nearly equivalent momenta and flow rates for the four streams are the major constraints of this technique [74].

3.4 Staggered herringbone and toroidal mixers

Unlike active mixers that depend on external sources to physically agitate the fluids, passive mixers achieve mixing by hydrodynamic manipulation of the fluids such as chaotic advection [75], fluid lamination [76], and sequential combining and splitting within the microchannels [77]. The staggered herringbone micromixer (SHM) is an innovative microchannel design which was developed as passive mixer in 2002 by Stroock et *al.* [78]. SHM has a transverse components consist of repeated patterns of groves in the microchannel that allow for reducing mixing length and generating chaotic flow (Figure 2G) [78]. Moreover, this design demonstrates a negligible flow resistance and higher diffusion rate in comparison to other designs with similar dimensions [78]. In addition, SHM can function efficiently at relatively low *Re* ($0 < R < 100$) which is beneficial in controlled microfabrication by microfluidic systems [78]. The fast and refined mixing performance of SHM can produce homogenous particle size of DDSs [32, 79]. Recently, split-and-recombine micromixer with dislocation sub-channels was presented by Li et *al*. [80] in 2013 as an alternative design to SHM. For *Re* in the range of 1-100 the dislocation sub-channel design improves mixing performance as a result of inertial collisions, multidirectional vortices and collision-induced flow in the mixing chambers [81]. Therefore, Precision NanoSystems Inc. adopted and modified this design to form the toroidal mixer (TrM) structure [79] (Figure 2H). In TrM, the rapid mixing is achieved by chaotic advection induced by generating more vortices and centrifugal forces that occurred between the columns within the microchannels [81]. Moreover, the new TrM design can scale-up production of DDSs (e.g., liposomes) from 12 mL/min (in SHM) to 200 mL/min which is very useful in pharmaceutical industry [79].

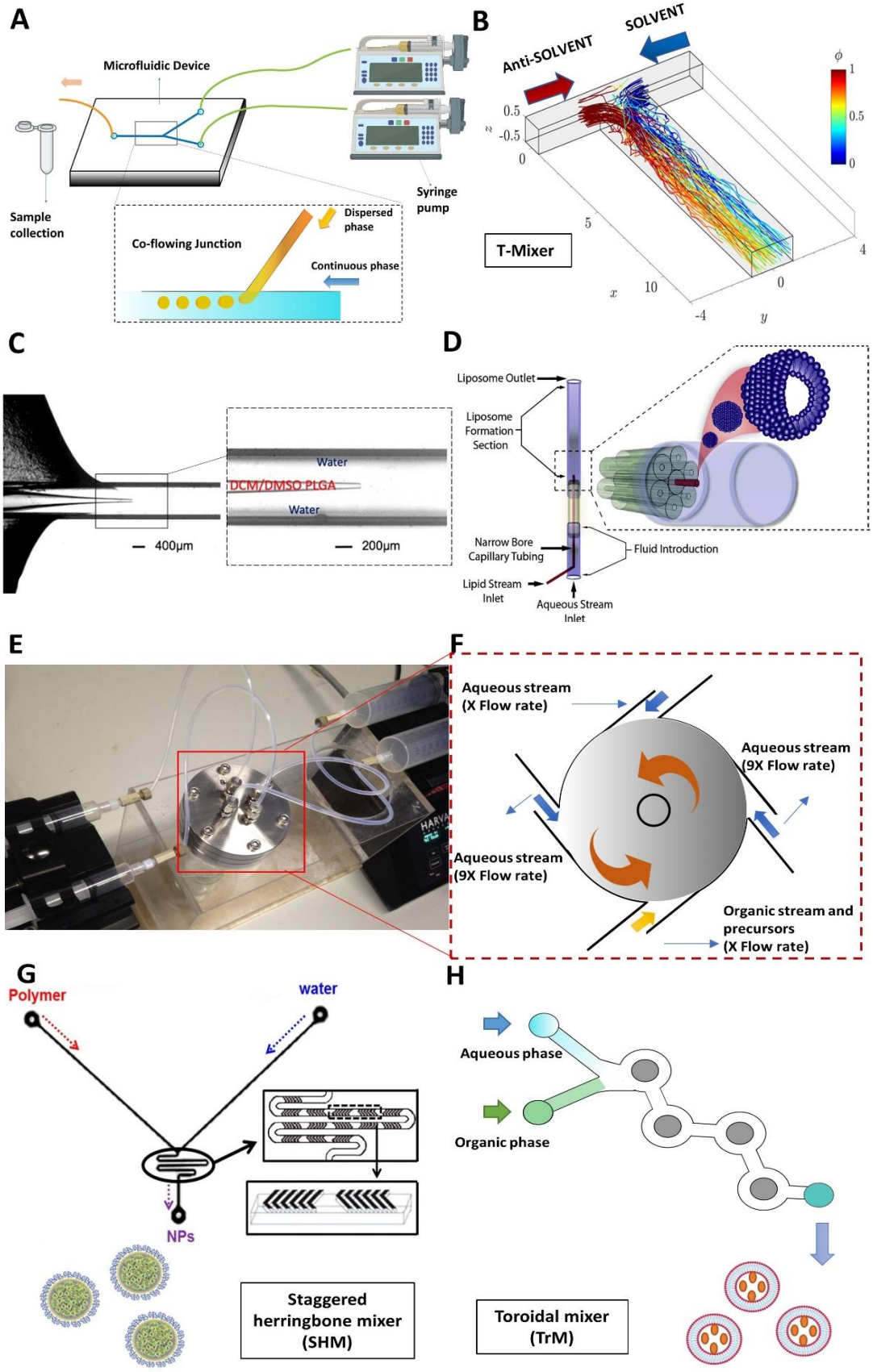

Figure 2. A) Schematic representation of basic microfluidic device and co-flowing junction. **B)** Three-dimensional representation of the T-mixer with coordinates normalized with the edge length of the inlet d = 0.001 m. Reprinted from [64] with permission from John Wiley and Sons. **C)** Optical microscopic image of coaxial microfluidic device (HFF) fabricated with glass capillaries. Reprinted from [12] with permission from Springer Nature under the

terms of the Creative Commons CC BY license. **D)** A glass multi-capillary array device for generating a 3D HFF stream. Reprinted from [72] with the permission from the Royal Society of Chemistry. **E)** Experimental setup for the solution and solvent stream mixing using MIVM device. Reprinted from [74] with the permission from Elsevier. **F)** Schematic showing the mixing conditions of the solution and solvent streams within MIVM. **G)** Schematic of a polymeric nanoparticle formulation strategy employing the staggered herringbone micromixer (SHM). Reprinted from [82] with the permission from ACS Publications. **H)** Schematic representation of Toroidal mixer (TrM) for formulating DDSs.

4 Microfluidic techniques control the properties of the DDSs

4.1 Size

The size uniformity and reproducibility of the nanoformulation are essential requirements for pharmaceutical applications. Controlling molecular assembly and particle growth (t_{agg}) plays the key role in obtaining the desirable size of DDSs. Studies revealed that the determinant factor for nucleation time is the precursors concentration in the microfluidic production of nanoformulations, while t_{agg} is govern by *Re*, total flow rate (TFR) and the flow rate ratio (FRR) between aqueous and organic phase [83, 84]. Increasing the FRR can reduces the mixing time which results in reducing the diameter of the liposomes prepared by HFF mixer [56, 57]. One or more of these parameters can be manipulated in the microfluidic system to achieve the required size range. For example, Ghazal et *al*. [35] has assessed the dependance of multilamellar vesicles (MLVs) size and monodispersity on HFF device geometry and FRRs [35]. This study found that FRR has a significant role in modulating the size distribution of the produced MLVs, while TFR exhibited much less impact (Figure 3A&B). Increasing the FRR from 10 to 50 at constant TFR (100 µL/min) results in 27% reduction in both mean size and PDI (Figure 3B). The design of the microfluidic chip has also shown a tangible effect on the MLVs size due to the impact of the channel length and geometry on difution [35]. Another study conducted by Lim et *al*. [85] investigated the impact of *Re* on various types of nanoparticle production including PLGA-PEG, lipid vesicles, iron oxide nanoparticles and polysterne nanoparticles [85]. This work has shown a significant reduction in the size of all tested formulation (from 150 to 20 nm) when *Re* was increased from 500 to 3500 [85]. These results implied that the size and PDI of nanoparticles can be easily controlled by microfluidic parameters.

4.2 Shape and structure

The shape of DDSs is one important factor for regulating cellular uptake and enhancing API encapsulation [86]. Moreover, modifying the structure such as increasing the porosity and pore size in NPs were associated with increasing the drug release rate. Mesoporous silica nanomaterial was successfully prepared using spiral-shaped microfluidic devices. By changing the flow rate, it was possible to transform the morphology of mesoporous silica from nanofibers to spherical nanoparticles [87]. In another research, the compactness of chitosan nanoparticles was tuned by applying different FRR and changing the hydrophobicity of the chitosan chains [88]. Liu et *al*. [89] has succesfuly prepared nanocarriers that enjoy desirable features including high stbility, biodegredability, pH-responsive and fast dissolution. These nanocarriers were fabricated by integrating sorafenib (SNF) or itraconazole (ICZ) nanocrystal drug core into a polymeric shell which made of acetylated dextran functionalized with folic acid (ADS-FA) using microfluidic platform (Figure 3C&D) [89].

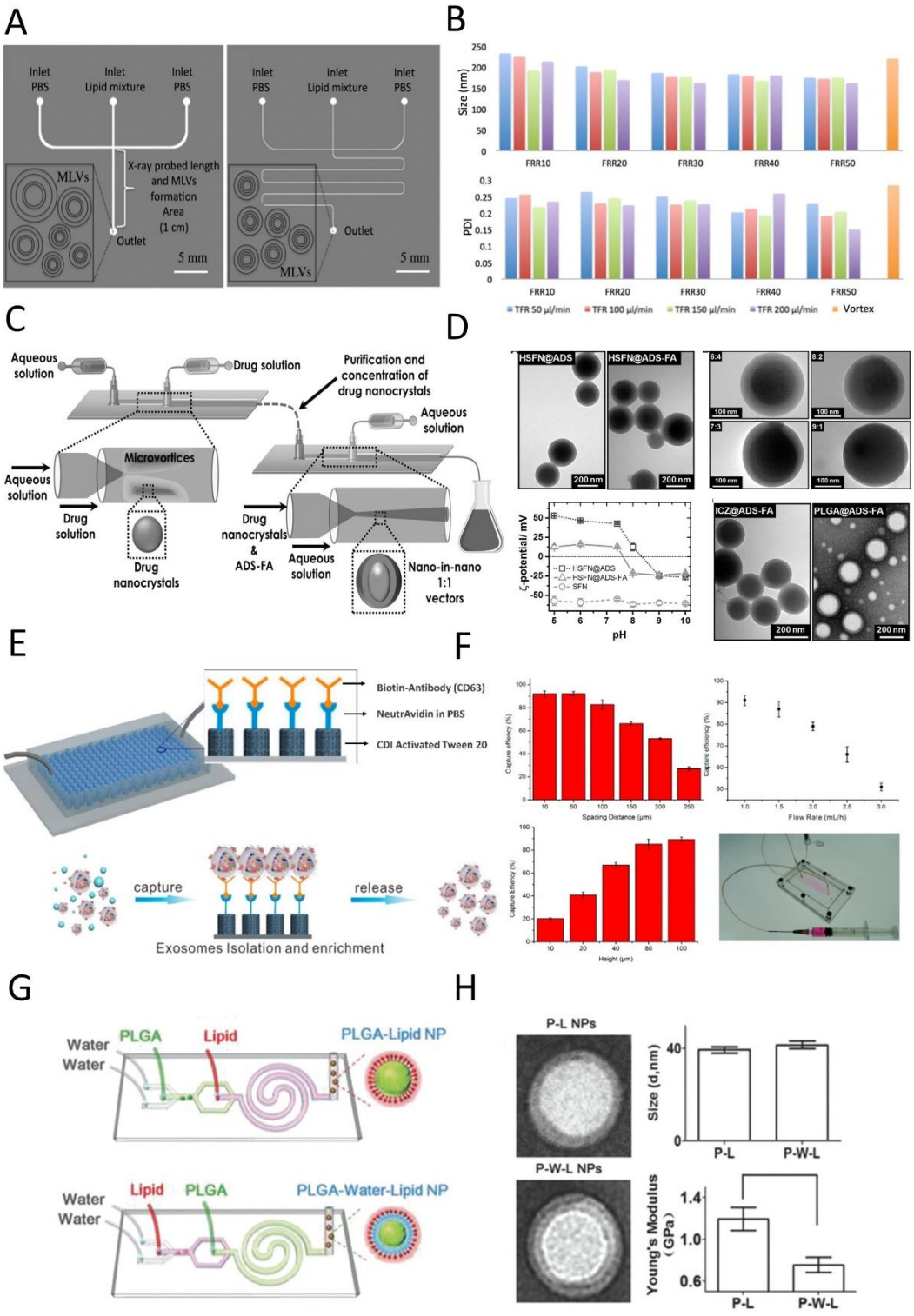

Figure 3. Examples of microfluidic fabrication of DDSs. **A)** A schematic representation of impact of two chip designs on the production of MLVs. **B)** DLS results for the MLVs produced showing the effects of FRR and TFR on size and polydispersity. Reprinted from [35] with the permission from ACS Publications. **C)** Schematics of the process to formulate the nano-in-nano vectors through the multistep microfluidic nanoprecipitation. **D)** TEM images of nano-vectors prepared by multistep microfluidic nanoprecipitation (HSFN@ADS) and (HSFN@ADS-FA), the effect of SFN and ADS-FA weight ratio (6:4 to 9:1) on shell thickness and ζ-Potential of SFN nanocrystals in terms of pH values of the dispersion media. Reprinted from [89] with the permission from John Wiley and Sons. **E)** Schematics describing the process of electroless plating and functionalizing MWCNT for capturing exosomes.

F) The effect of pillars height, pillars spacing distance and the flow rate on the capturing efficiency. Reprinted from [37] with the permission from the American Chemical Society. **G)** Assembling PLGA–lipid nanoparticles with varying amounts of interfacial water to modify the particle rigidity, P-L nanoparticles (without interfacial water layer, top) and P-W-L nanoparticles (with interfacial water layer, bottom). **H)** Size and Young's modulus of P-L nanoparticles and P-W-L nanoparticles from TEM and AFM scanning. Reprinted from [90] with the permission from John Wiley and Sons.

4.3 Surface engineering

One of the most common approach for improving the targetability of DDSs to cancer cells is surface modification. For example, Di Santo et *al.* [20] prepared hybrid nanoparticles consisting of graphene oxide (GO) flakes coated with cationic lipids using microfluidic mixing. The resulting particles had size of (>150 nm) and charge of (ξ = +15 mV) that are suitable for delivering plasmid DNA (pDNA) to human cervical cancer cells (HeLa) and human embryonic kidney (HEK-293) cells [20]. One of the challenges in fabricating functionalized nanocarriers is the lack of approaches for isolation and purification. In a study conducted by Wang et *al*. [37], chemically modified exosomes were prepared for active targeted drug delivery to cancer cells [37]. This study used three-dimensional (3D) nanostructured microfluidic chip consist of an ordered series of micropillars functionalized with multiwall carbon nanotubes (MWCNTs) to efficiently capture exosomes [37]. Capture efficiency can be optimized by changing height, spacing distances and flow rate (Figure 3E&F).

4.4 Elasticity

Recent studies have found that the mechanical properties such as elasticity of the DDSs have a significant influence on cellular uptake, drug release, and stability [5]. The precise manipulation of the flow and flow regime within the microfluidic system can modify the particle elasticity. Sun et *al*. [90] designed nanocarriers made of polymeric core (PLGA) and lipid shell with tuneable rigidity for regulating cellular uptake (Figure 3G&H) [90]. In this study, the particle elasticity was modulated in the microfluidics device by altering the injection order of organic solutions containing PLGA and lipid-PEG. This technique allows for variation in the water content leading to variation in Young's modulus which influences the internalization mechanism in Hela cells [90].

5 Applications of microfluidic techniques in drug delivery

5.1 Double and multiple emulations

Emulations are formed by mixing two immiscible liquid phases (dispersed phase & continuous phase) [91]. One of the common formulations in drug delivery are based on forming and stabilizing droplets within another droplets which is known as multiple emulsions. When small droplets are nested one inside the next, the formulation is called double emulsions [30]. This approach is highly applicable in pharmaceuticals and food products due to its ability to manipulate the properties of wide range of sensitive ingredients loaded into emulations [92]. Drug encapsulation and release kinetics can be regulated by controlling the size and size distribution, using stimuli-responsive materials and changing the shell thickness of the core-shell structures [93]. Conventional high-shear emulsification techniques have many disadvantages such as large polydispersity, structural variability and inconsistent encapsulation efficiency [93]. To overcome these limitations, researchers have developed an alternative protocol by using droplet microfluidics to formulate highly controllable multiple emulsions or emulsion-based templets for producing uniform particles in a single step. By balancing the interfacial

tension forces with the viscous forces, it is possible to produce uniform and versatile emulsion droplets with a coefficient of variation (CV) of less than 5% [94]. Michelon et *al*. [95] produced W/O/W double emulsions as templets for forming β-carotene-loaded liposomes using capillary microfluidic device [95]. These liposomes showed controllable size distribution and relatively good stability for over 7 days [95]. Jeong et *al*. [96] developed 3D HFF microfluidic device which was carefully set up to produce multiple emulsion droplets with tunable morphologies [96]. By combining the diffusion-induced phase separation with evaporation-induced self-assembly (EISA), it was possible to continuously synthesise hollow silica spheres which contain a single core or multiple cores (Figure 4) [96].

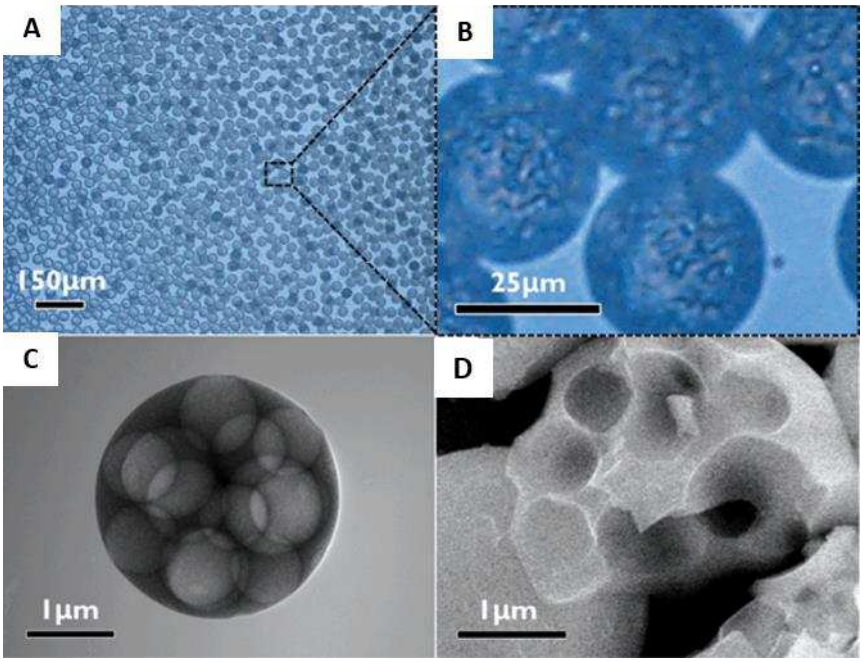

Figure 4. (A, B) Optical micrographs of monodisperse double emulsions with many fine internal droplets. STEM **(C)**, and SEM **(D)** images of the resultant hollow particles with multiple cores. Reprinted from [96] with permission from the Royal Society of Chemistry.

5.2 Protein-based nanocarriers

Potential toxicity and lack of biodegradability of may synthetic polymers have encouraged researcher to utilize natural biomaterial as an alternative building block for several DDSs [6, 97]. However, processing biomaterials such as silk fibroin (SF), collagen and gelatin is more challenging due to the complexity and sensitivity of the protein-based materials [18, 98]. Hardin et *al*. [99] have used a capillary microfluidic device to prepare uniformly sized gelatin microparticles [99]. These microspheres served as template for adsorbing DNA-functionalized polystyrene which facilitate DNA release under different thermal conditions [99]. Processing conditions can affect the properties and reproducibility of the produced protein nanoparticles. A recent study conducted by Solomun et *al*. [100] investigated the impact of precise control of SF nanoparticles manufacture assisted by microfluidics [100]. Although no substantial difference in particle size was observed between manual and microfluidic mixing method, significant reduction in the surface charge (−41 mV to −29 mV) was reported [100]. Wongpinyochit et *al*. [32] has tested the influences of microfluidic device parameters such as TFR and FRR on the SF particle size and shape. SHM (NanoAssemblr™ benchtop instrument) was used in this study to produce SF particles by desolvation method using two organic solvents (acetone & isopropanol) (Figure 5). High

organic solvent: aqueous ratio (i.e., isopropanol: water = 5:1) combined with relatively low TFR (1 mL/min) has shown significantly higher yield in comparison to other conditions. In addition, particle size, polydispersity and surface charge can be tuned by modifying TFR (1- 12 mL/min), FRR (1:1, 3:1, 5:1) and changing the organic solvent (Figure 5) [32]. The variety of tunable conditions in this microfluidic device allow for precise optimization of properties of the produced nanoparticles.

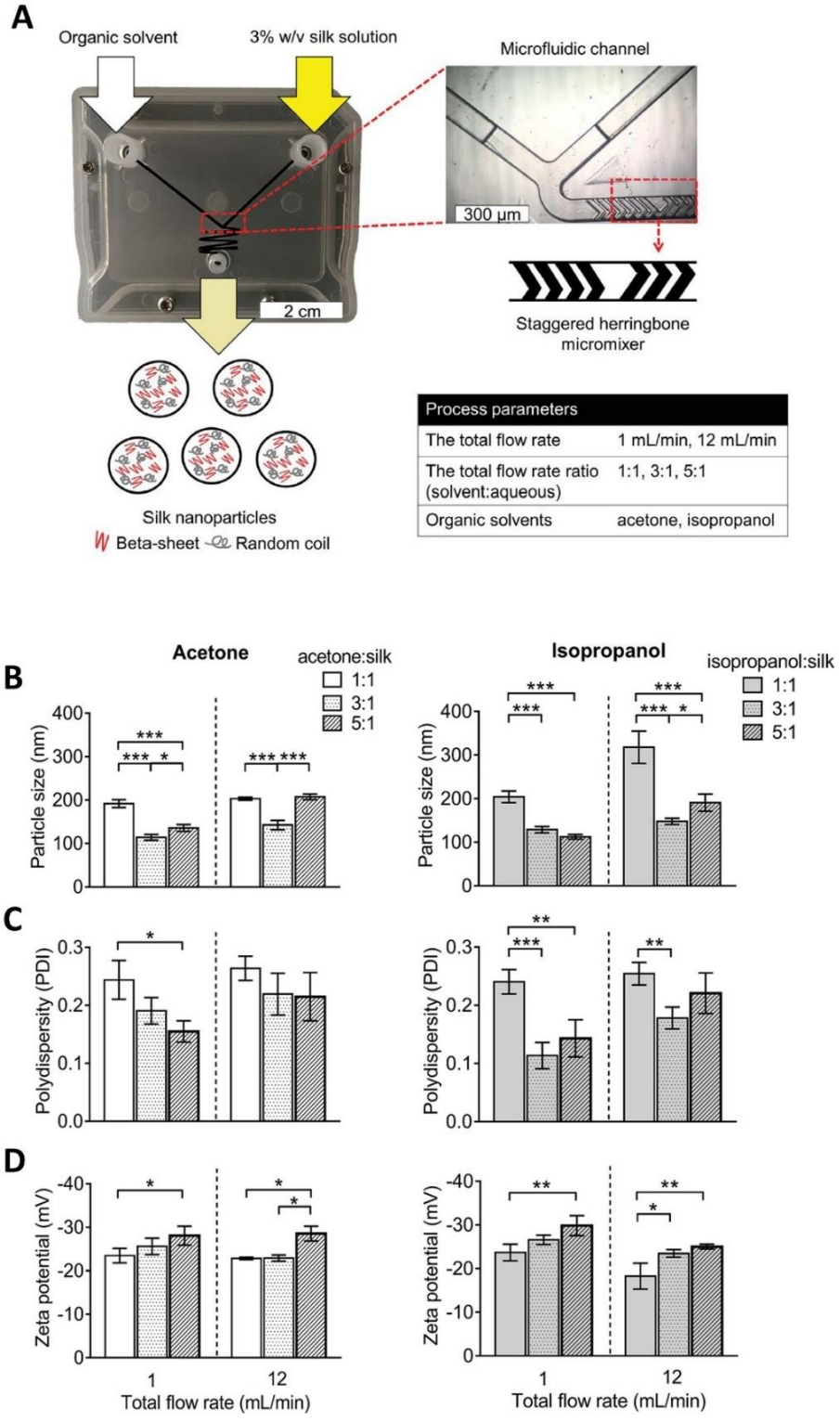

Figure 5. Microfluidic fabrication of protein-based nanocarriers. **A)** Organic solvent and SF solution were pumped into two inlets and rapidly mixed (NanoAssemblr™ benchtop instrument) at different TFR & FRR to form silk

nanoparticles by nanoprecipitation. The cartridge contains Y-junction and a staggered herringbone structure. **B)** particle size, **C)** polydispersity index (PDI), and **D)** zeta potential of silk nanoparticles. Reprinted from [32] with permission from the Royal Society of Chemistry under the terms of the Creative Commons CC BY license.

5.3 Lipid-based nanoparticles

Lipid nanoparticles (LNPs), including liposomes, have served as DDSs for many APIs and food ingredients due to their ability to load the cargo within the lipid shell or the particle core [34, 101]. Despite the multiple advantages conventional LNPs hold such as biocompatibility and high loading efficiency, further improvements are required to increase their clinical applications [102, 103]. The most common strategy to improve the LNPs formulations is surface modification that results in enhancing stability, increasing retention time in blood and delivering drugs and genes to the targeted tissues [102, 104-106]. Conventional methods to prepare lipid-based nanomaterials are based on lipid layer hydration or bulk mixing of several liquid phases, leading to the formation of inhomogeneous nanoparticles. Several LNP formulations have been developed using microfluidic devises to address the limitations of the conventional LNP production methods. The principle of LNP production by microfluidic platforms is similar to some of the conventional methods such as hydration and organic solvent injection. Utilization of fluid dynamics mixing, the interface of the microfluidic devices and the shape of the microfluidic channels effectively assisted the production of the LNPs with desirable properties [34, 107, 108]. Kitazoe et *al*. [109] designed a microfluidic device with one inlet and 13 outlets to produce LNPs encapsulating pDNA. In this study, lipid films blended with cationic polymer (Polylysine) were coated on the inner surface of the glass channels before injecting pDNA to hydrate the lipid film. LNPs were formed and the loading of the pDNA was achieved by electrostatic interactions. This microfluidic technique not only produce uniform NLPs but also significantly shorten the production time [109]. Another study conducted by Nakamura et *al*. [110] used herringbone chaotic mixer to prepare pH-sensitive LNPs (30, 100, 200 nm) for targeting lymph nodes (LNs) [110]. This work assessed the effect of the particle size and charge on the transitivity to and distribution within LNs (Table 1). The small size of these LNPs (30 nm) resulted in significantly higher transitivity to LNs when injected subcutaneously in mice. On the other hand, the negatively charged LNPs were transported more efficiently to LNs than neutral and positively charge batches [110]. Balbino et *al.* [3] prepared cationic liposomes using single and double HFF technique for gene delivery to Hela cells [3]. In this study, the lipid concentration and FRR were manipulated for producing liposomes (250-530 nm) with polydispersity ranging from 0.29 to 0.87 to encapsulate pDNA [3]. The single and double HFF devices used in this study produced unilamellar liposomes that enhanced the biological efficiency of pDNA[3].

5.4 Polymeric and hybrid nanoparticles

Polymer-based micro and nanoparticles can be prepared using several conventional methods including crosslinking, ionic gelation, solvent evaporation, and solvent-antisolvent mixing [111]. Similar to the other discussed nanoformulations, polymeric particles can be fabricated by rapid mixing within microfluidic systems with higher degree of controllability and uniformity in comparison to other methods. HFF and droplet-based methods are among the most common microfluidic system to produce several polymeric particles for the delivery of wide range of drugs such as amoxicillin [112], docetaxel [113], dexamethasone [114] (Table 1). Droplet based microfluidics can assist the production of spherical and non-spherical microparticles through ionic crosslinking to modify the drug release kinetics. For example, alginate microgels were generated in three different shapes (spherical, tailed & mushroom-like microgel) by modifying the microfluidic device where the ionic crosslinking takes

place (Table 1) [115]. This study found the manipulating the morphology of the microgels affects the release behaviour of the loaded drug (iopamidol) [115]. In gene delivery, Koh et *al*.[116] efficiently produced polyethylenimine (PEI) and pDNA complexes using HFF device [116]. The laminar flow formed in the HFF chip created well-defined interfacial region which allowed for generating ordered condensates of PEI/pDNA. These PEI/pDNA complexes have demonstrated an improved size control, higher gene transfection efficiency and lower cytotoxicity in mouse NIH 3T3 fibroblast cells and mouse embryonic stem (mES) cells in comparison to bulk mixing methods [116].

HFF microfluidic reactor was successfully used to fabricate β-carotene-Pluronic F127 by rapid nanoprecipitation [117]. Compare to bulk mixing, rabid mixing generated by HFF allows for the formed β-carotene nuclei to be efficiently coated and stabilized by Pluronic F127 molecules [117]. Another study used as simple T-mixer design to generate Janus nanoparticles and monophasic nanoparticles comprised of PLGA through fast nanoprecipitation [118]. Both nanoparticle types were used to encapsulate anticancer agents such as paclitaxel (PTX) and doxorubicin (DOX) and demonstrated different release profiles for each drug [118]. In another study conducted by Hong et *al*. [119] spherical polyester-based nanoparticles were prepared by herringbone mixer with sizes ranging from 50 to 150 nm depending on TFR and FRR [119]. These particles have a dual enzymatic stimuli-responsive polyester due to the ester bonds and sulfide linkages fabricated by the microfluidic system. Moreover, coating these particles with stabilizers such as PEG enhanced the viability and reduced toxicity to Hela cells [119].

Table 1. Recent examples of DDSs fabricated by microfluidic platforms

Microfluidic devices	Formulations	DDS types	Size (nm)	Loaded cargo	Advantages	Refs
T-Mixer	NA	Small molecule NPs	50-120	Ibuprofen	Controllable size & narrow size distribution	63
T-Mixer	PLGA[1]	Janus & Monophasic NPs	100-200	Paclitaxel & doxorubicin	Multiple payloads & modified drug release profile	118
Y- Junction	NA	Amorphous NPs	450	Cefuroxime axetil	Enhanced drug dissolution rate & controllable size	120
Y- Junction	NA	Small molecule NPs	364	Danazol	Enhanced drug dissolution rate & controllable size	121
Y- Junction	Graphene oxide (GO)/DOTAP	Lipid NPs	<150	pDNA	Uniformly coating GO sheets with lipid layers that is suitable for gene delivery	20
Turbulent jet mixer	PLGA -PEG[2]	Polymeric NPs	~100	Docetaxel	Versatile and controlled preparation of NPs & high production rates	85
2D-HFF	HMCS[3]	Polymeric NPs	74-216	paclitaxel	Narrow size distribution, high loading capacity, and controlled compactness	88
2D-HFF	PMOXA-PDMS-PMOXA[4]	Micelles	20-100	Tamoxifen	Controllable size & polydispersity	122
2D-HFF	Poloxamer 407	Polymeric micelles	75	Mithramycin	Low polydispersity, robustness & high reproducibility	71

2D-HFF	HPMCAS[5] polymer	Microspheres	~5000	Atorvastatin & Celecoxib	Narrow size distribution and pH responsive dissolution behaviour	[123]
2D-HFF	CAMs (Au nanorods)	Vesicles	500-2000	Rhodamine B	Controllable dimension and the morphology	[124]
2D-HFF	Sodium alginate	Microgel particles	>5000	Iopamidol	Shape-dependent release	[115]
2D-HFF	Sodium alginate	Microgel NPs	>5000	Ampicillin	pH-responsive & shape-dependent release	[125]
2D-HFF	Polyethylenimine (PEI)	Polymeric NPs	~250	pDNA	Narrow size distribution & enhanced transfection efficiency	[116]
3D-HFF	PLGA -PEG	Polymeric NPs	13-150	Docetaxel	Tunable properties & high production rates for *in vivo* study	[27]
3D-HFF	PLGA	Polymeric NPs	35-350	Dexamethasone	Enhanced drug loading & controllable particle size	[114]
3D-HFF	Silica-PMMA[6]	Multiple emulsions	>1000	NA	Precise control over droplet size and the internal morphology	[96]
MIVM	PEG-PLA[7]	Polymeric NPs	80-200	Curcumin	Controllable size & narrow size distribution	[74]
Toroidal mixer	DSPC/Chol/DOPS	Liposomes	50-70	Ovalbumin	Narrow size distribution & high production rates	[79]
Herringbone Mixer	DOPC/POPC/Chol/PEG-DMG	Lipid NPs	20-100	siRNA	Controllable size & narrow size distribution	[84]
Herringbone Mixer	Silk fibroin	Polymeric NPs	100-300	NA	High particle yield & tunable properties	[32]
Herringbone Mixer	DOTAP/ cholesterol/ DMG-PEG	Lipid NPs	30-200	DiD (lipophilic tracer)	pH-responsive & size-dependent transitivity to lymph nodes	[110]
Herringbone Mixer	DMAP-BLPa/DSPC/cholesterol/PEG-DMG	Lipid NPs	30-110	siRNA	Size-dependent pharmacokinetics & gene silencing potency	[126]
Herringbone Mixer	DOPE/DOTAP, DOPE/DDA	Liposomes	50-750	Dil-C18 (lipophilic tracer)	Controllable size & size-dependent *in vitro* cellular uptake	[127]

Abbreviations:1 poly(lactic-co-glycolic acid), 2 Polyethylene glycol, 3 Hydrophobically modified chitosan, 4 poly(2-methyl-2-oxazoline)-*block*-poly(dimethylsiloxane)-*block*-poly(2-methyl-2-oxazoline, 5 hydroxypropyl methylcellulose acetate succinate, 6 poly(methyl methacrylate, 7 Poly (DL-lactide).

6 Industrial application

Pharmaceutical products have a very high value with estimated global market of one trillion US$ [128]. However, the process required from discovery, formulation to manufacturing the final product is costly and time consuming [128]. Therefore, one of the main priorities of pharmaceutical companies is to implement new strategies for rapid and controlled manufacturing of pharmaceutical products to achieve cost effectiveness, sustainability and on-demand production [129]. In microfluidics, the translation form bench-top instrument to the industrial scale requires high production rate and compliance with good manufacturing practice (GMP)[79]. Increasing the production rate by increasing the fluid velocity within the microfluidic channel is undesirable due to the significant increase in the pressure drop across the fabrication device. Therefore, generating a cumulative flow by increasing the number of identical devices at the same fluid velocity is a better alternative strategy for production at

industrial level [9, 130]. In addition, using a multiple pressure sources (pumps) for each microfluidic device can provide more control, thus more uniform size distribution but it is not cost-efficient. Distributing a uniform flow from a main pressure source is more convenient and practical for industrial applications and substantial research and development are required in this area [71, 131, 132]. NanoAssembler GMP system is one of the recent development in large scale production of pharmaceutical formulations using microfluidic platforms[79]. This system offers a replaceable cartridge, which has the mixing elements, and is equipped with custom pumps. Changing the cartridge is not only beneficial for maintaining the mixing quality and sterility, but also allows for switching the mixer type (SHM & TrM)[79]. Switching to continuous flow production using microfluidics still has many challenges in regard to quality control and cost efficiency. By implementing new approaches and modifying the current designs, microfluidics can play a key role in large scale production of pharmaceuticals, especially in nanomedicine.

7 Conclusion

The recent innovations and developments in the microfluidic technology have offered a better alternative to many conventical techniques for designing and producing DDSs. The new designs of microfluidic systems have many functionalities that address many of limitations of the early designs. This substantial improvement has made microfluidic platform an effective tool in fabricating a wide range of formulations for drug and gene delivery. The main challenges that complicated the formulation development in the field of nanomedicine are reproducibility and manipulation of the properties. These challenges slow down the translation of many potentially effective DDSs form academia to large scale production in the pharmaceutical industry. Most of the nanoformulations that are designed as DDSs for many drugs and genetic material are fabricated by fast nanoprecipitation or self-assembly. Both methods are difficult to control in conventional bulk methods leading to lack of uniformity of the produced particles and large batch-to-batch variation. However, the rapid mixing, which occurs in the channels of the microfluidic device, allows for predetermined conditions that control size, shape and reproducibility. Manipulating the production parameters and the geometric design can not only change the flow regime of the mixed fluids but also modify or create specific properties in the formed DDSs. These properties include size, shape, surface charge, elasticity and pre-programmed release profile of the laded cargos. Various types of DDSs such as multiple emulsions, protein-based particles, lipid and polymeric nanoparticles, have been successfully produced by several microfluidic strategies. The advantages provided by these DDSs improves the delivery and the therapeutic quality of many APIs especially anticancer agents.

8 Future perspectives

There are many hurdles for microfluidic technologies to become widely applicable in the pharmaceutical industry. In many cases, a specific geometric design of the microfluidic channels is manufactured and calibrated to fabricate specific formulation (e.g. double and multiple emulations) which might not be suitable for controlling the assembly process of other types of DDSs (e.g. polymeric nanoparticles). Despite the flexibility of operating parameters (TFR & FRR) provided by the microfluidic platform, it is still difficult to assemble some types DDSs in a single step. For example, layer-by-layer assembly and coating protocols [133-135] require completely different mixing conditions from fast nanoprecipitation. Due to the micrometric dimensions of the microfluidic channels and high TFR that pass through, impurities and precipitates can accumulate in the channels which can alter the mixing

conditions. To ensure that the mixing channels are free from any impurities and in a perfect condition, NanoAssemblr™ have designed a benchtop instrument with disposable chips to obtain precise DDSs properties in every single batch. However, this approach can be expensive and allows for limited mixer designs. Another area for improvement in the current microfluidic designs is real time characterization techniques. These techniques can help optimizing the microfluidic parameters and directly monitor any change in DDSs formation. Recently, studies have used advanced on-chip characterization techniques such as dynamic light scattering (DLS) [136], confocal Raman microscopy [137] and fluorescence resonance energy transfer (FRET) [138]. However, further investigation is required to improve current designs to obtain more accurate on-chip data during microfabrication of DDSs. Although difficulties such as the cost and complexity still remain in some current designs, microfluidic technologies demonstrate an enormous potential as practical methods for DDSs large scale production. In-depth understanding of the mixing principles in combination with comprehensive evaluation of the current systems can lead to the development of a new generation of microfluidic devices that accelerate the translation of many novel DDSs formulation to the pharmaceutical market.

Acknowledgements

The authors would like to thank EPSRC (EP/N007174/1 and EP/N023579/1), The Royal Society (RG160662), and Jiangsu specially appointed professor program for support.

Reference:

1. Valencia, P. M.; Farokhzad, O. C.; Karnik, R.; Langer, R., Microfluidic technologies for accelerating the clinical translation of nanoparticles. *Nat Nanotechnol* **2012,** *7* (10), 623-9.
2. Patra, J. K.; Das, G.; Fraceto, L. F.; Campos, E. V. R.; Rodriguez-Torres, M. d. P.; Acosta-Torres, L. S.; Diaz-Torres, L. A.; Grillo, R.; Swamy, M. K.; Sharma, S.; Habtemariam, S.; Shin, H.-S., Nano based drug delivery systems: recent developments and future prospects. *Journal of Nanobiotechnology* **2018,** *16* (1), 71.
3. Balbino, T. A.; Aoki, N. T.; Gasperini, A. A. M.; Oliveira, C. L. P.; Azzoni, A. R.; Cavalcanti, L. P.; de la Torre, L. G., Continuous flow production of cationic liposomes at high lipid concentration in microfluidic devices for gene delivery applications. *Chemical Engineering Journal* **2013,** *226*, 423-433.
4. Sanjay, S. T.; Zhou, W.; Dou, M.; Tavakoli, H.; Ma, L.; Xu, F.; Li, X., Recent advances of controlled drug delivery using microfluidic platforms. *Advanced Drug Delivery Reviews* **2018,** *128*, 3-28.
5. Hui, Y.; Yi, X.; Hou, F.; Wibowo, D.; Zhang, F.; Zhao, D.; Gao, H.; Zhao, C.-X., Role of Nanoparticle Mechanical Properties in Cancer Drug Delivery. *ACS Nano* **2019,** *13* (7), 7410-7424.
6. Su, C.; Liu, Y.; Li, R.; Wu, W.; Fawcett, J. P.; Gu, J., Absorption, distribution, metabolism and excretion of the biomaterials used in Nanocarrier drug delivery systems. *Advanced Drug Delivery Reviews* **2019,** *143*, 97-114.
7. Wicki, A.; Witzigmann, D.; Balasubramanian, V.; Huwyler, J., Nanomedicine in cancer therapy: Challenges, opportunities, and clinical applications. *Journal of Controlled Release* **2015,** *200*, 138-157.
8. Köstler, S.; Ribitsch, V., Synthetic Approaches to Organic Nanoparticles. Weinheim, Germany: Wiley‐VCH Verlag GmbH & Co. KGaA: Weinheim, Germany, 2007.
9. Capretto, L.; Carugo, D.; Mazzitelli, S.; Nastruzzi, C.; Zhang, X., Microfluidic and lab-on-a-chip preparation routes for organic nanoparticles and vesicular systems for nanomedicine applications. *Advanced drug delivery reviews* **2013,** *65* (11-12), 1496-1532.
10. Nadrian, C. S.; Hanadi, F. S., DNA nanotechnology. *Nature Reviews Materials* **2017,** *3* (1).
11. Zhang, H.; Zhu, Y.; Shen, Y., Microfluidics for cancer nanomedicine: from fabrication to evaluation. *Small* **2018,** *14* (28), 1800360.

12. Xu, J.; Zhang, S.; Machado, A.; Lecommandoux, S.; Sandre, O.; Gu, F.; Colin, A., Controllable microfluidic production of drug-loaded PLGA nanoparticles using partially water-miscible mixed solvent microdroplets as a precursor. *Scientific reports* **2017,** *7* (1), 1-12.
13. Song, W.; Gregory, D. A.; Al-Janabi, H.; Muthana, M.; Cai, Z.; Zhao, X., Magnetic-silk/polyethyleneimine core-shell nanoparticles for targeted gene delivery into human breast cancer cells. *Int J Pharm* **2019,** *555*, 322-336.
14. Song, W.; Muthana, M.; Mukherjee, J.; Falconer, R. J.; Biggs, C. A.; Zhao, X., Magnetic-Silk Core–Shell Nanoparticles as Potential Carriers for Targeted Delivery of Curcumin into Human Breast Cancer Cells. *ACS Biomater Sci Eng* **2017,** *3* (6), 1027-1038.
15. Zhao, X.; Pan, F.; Zhang, Z.; Grant, C.; Ma, Y.; Armes, S. P.; Tang, Y.; Lewis, A. L.; Waigh, T.; Lu, J. R., Nanostructure of Polyplexes Formed between Cationic Diblock Copolymer and Antisense Oligodeoxynucleotide and Its Influence on Cell Transfection Efficiency. *Biomacromolecules* **2007,** *8* (11), 3493-3502.
16. Zhao, X.; Zhang, Z.; Pan, F.; Waigh, T. A.; Lu, J. R., Plasmid DNA complexation with phosphorylcholine diblock copolymers and its effect on cell transfection. *Langmuir* **2008,** *24*, 6881-6888.
17. Zhao, X.; Pan, F.; Holt, C. M.; Lewis, A. L.; Lu, J. R., Controlled Delivery of Antisense Oligonucleotides (ASOs): a Brief Review of Current Strategies. *Expert Opin. Drug Deliv.* **2009,** *6*, 673-686.
18. Tomeh, M. A.; Hadianamrei, R.; Zhao, X., Silk Fibroin as a Functional Biomaterial for Drug and Gene Delivery. *Pharmaceutics* **2019,** *11* (10), 494.
19. Nishiyama, N.; Kataoka, K., Current state, achievements, and future prospects of polymeric micelles as nanocarriers for drug and gene delivery. *Pharmacology & Therapeutics* **2006,** *112* (3), 630-648.
20. Di Santo, R.; Digiacomo, L.; Palchetti, S.; Palmieri, V.; Perini, G.; Pozzi, D.; Papi, M.; Caracciolo, G., Microfluidic manufacturing of surface-functionalized graphene oxide nanoflakes for gene delivery. *Nanoscale* **2019,** *11* (6), 2733-2741.
21. Murday, J. S.; Siegel, R. W.; Stein, J.; Wright, J. F., Translational nanomedicine: status assessment and opportunities. *Nanomedicine: Nanotechnology, Biology and Medicine* **2009,** *5* (3), 251-273.
22. Johnson, B. K.; Prud'homme, R. K., Mechanism for Rapid Self-Assembly of Block Copolymer Nanoparticles. *Physical Review Letters* **2003,** *91* (11), 118302.
23. Gindy, M. E.; Panagiotopoulos, A. Z.; Prud'homme, R. K., Composite block copolymer stabilized nanoparticles: simultaneous encapsulation of organic actives and inorganic nanostructures. *Langmuir* **2008,** *24* (1), 83-90.
24. Abou‐Hassan, A.; Bazzi, R.; Cabuil, V., Multistep continuous‐flow microsynthesis of magnetic and fluorescent γ‐Fe2O3@ SiO2 core/shell nanoparticles. *Angewandte Chemie* **2009,** *121* (39), 7316-7319.
25. Zhang, L.; Feng, Q.; Wang, J.; Sun, J.; Shi, X.; Jiang, X., Microfluidic synthesis of rigid nanovesicles for hydrophilic reagents delivery. *Angewandte Chemie* **2015,** *127* (13), 4024-4028.
26. Demello, A. J., Control and detection of chemical reactions in microfluidic systems. *Nature* **2006,** *442* (7101), 394-402.
27. Lim, J.-M.; Bertrand, N.; Valencia, P. M.; Rhee, M.; Langer, R.; Jon, S.; Farokhzad, O. C.; Karnik, R., Parallel microfluidic synthesis of size-tunable polymeric nanoparticles using 3D flow focusing towards in vivo study. *Nanomedicine: Nanotechnology, Biology and Medicine* **2014,** *10* (2), 401-409.
28. Leung, M. H. M.; Shen, A. Q., Microfluidic assisted nanoprecipitation of PLGA nanoparticles for curcumin delivery to leukemia jurkat cells. *Langmuir* **2018,** *34* (13), 3961-3970.
29. Chen, D.; Love, K. T.; Chen, Y.; Eltoukhy, A. A.; Kastrup, C.; Sahay, G.; Jeon, A.; Dong, Y.; Whitehead, K. A.; Anderson, D. G., Rapid Discovery of Potent siRNA-Containing Lipid Nanoparticles Enabled by Controlled Microfluidic Formulation. *Journal of the American Chemical Society* **2012,** *134* (16), 6948-6951.

30. Clegg, P. S.; Tavacoli, J. W.; Wilde, P. J., One-step production of multiple emulsions: microfluidic, polymer-stabilized and particle-stabilized approaches. *Soft Matter* **2016,** *12* (4), 998-1008.
31. Feng, H.; Zheng, T.; Li, M.; Wu, J.; Ji, H.; Zhang, J.; Zhao, W.; Guo, J., Droplet-based microfluidics systems in biomedical applications. *ELECTROPHORESIS* **2019,** *40* (11), 1580-1590.
32. Wongpinyochit, T.; Totten, J. D.; Johnston, B. F.; Seib, F. P., Microfluidic-assisted silk nanoparticle tuning. *Nanoscale Advances* **2019,** *1* (2), 873-883.
33. Montoya, N. V.; Peterson, R.; Ornell, K. J.; Albrecht, D. R.; Coburn, J. M., Silk Particle Production Based on Silk/PVA Phase Separation Using a Microfabricated Co-flow Device. *Molecules* **2020,** *25* (4), 890.
34. Maeki, M.; Kimura, N.; Sato, Y.; Harashima, H.; Tokeshi, M., Advances in microfluidics for lipid nanoparticles and extracellular vesicles and applications in drug delivery systems. *Adv Drug Deliv Rev* **2018,** *128*, 84-100.
35. Ghazal, A.; Gontsarik, M.; Kutter, J. P.; Lafleur, J. P.; Ahmadvand, D.; Labrador, A.; Salentinig, S.; Yaghmur, A., Microfluidic Platform for the Continuous Production and Characterization of Multilamellar Vesicles: A Synchrotron Small-Angle X-ray Scattering (SAXS) Study. *The Journal of Physical Chemistry Letters* **2017,** *8* (1), 73-79.
36. Amoyav, B.; Benny, O., Controlled and tunable polymer particles' production using a single microfluidic device. *Applied Nanoscience* **2018,** *8* (4), 905-914.
37. Wang, J.; Li, W.; Zhang, L.; Ban, L.; Chen, P.; Du, W.; Feng, X.; Liu, B.-F., Chemically Edited Exosomes with Dual Ligand Purified by Microfluidic Device for Active Targeted Drug Delivery to Tumor Cells. *ACS applied materials & interfaces* **2017,** *9* (33), 27441-27452.
38. Liu, Z.; Fontana, F.; Python, A.; Hirvonen, J. T.; Santos, H. A., Microfluidics for Production of Particles: Mechanism, Methodology, and Applications. *Small* **2020,** *16* (9), n/a-n/a.
39. D'Addio, S. M.; Prud'homme, R. K., Controlling drug nanoparticle formation by rapid precipitation. *Advanced Drug Delivery Reviews* **2011,** *63* (6), 417-426.
40. LaMer, V. K.; Dinegar, R. H., Theory, production and mechanism of formation of monodispersed hydrosols. *Journal of the American Chemical Society* **1950,** *72* (11), 4847-4854.
41. Saad, W. S.; Prud'homme, R. K., Principles of nanoparticle formation by flash nanoprecipitation. *Nano Today* **2016,** *11* (2), 212-227.
42. Tao, J.; Chow, S. F.; Zheng, Y., Application of flash nanoprecipitation to fabricate poorly water-soluble drug nanoparticles. *Acta pharmaceutica sinica B* **2019,** *9* (1), 4-18.
43. Karnik, R.; Gu, F.; Basto, P.; Cannizzaro, C.; Dean, L.; Kyei-Manu, W.; Langer, R.; Farokhzad, O. C., Microfluidic platform for controlled synthesis of polymeric nanoparticles. *Nano letters* **2008,** *8* (9), 2906-2912.
44. Zhao, X.; Bian, F.; Sun, L.; Cai, L.; Li, L.; Zhao, Y., Microfluidic Generation of Nanomaterials for Biomedical Applications. *Small* **2020,** *16* (9), 1901943.
45. Johnson, B. K.; Prud'homme, R. K., Chemical processing and micromixing in confined impinging jets. *AIChE Journal* **2003,** *49* (9), 2264-2282.
46. Batchelor, C. K.; Batchelor, G. K., *An introduction to fluid dynamics*. Cambridge university press: 2000.
47. Nguyen, N.-T.; Wereley, S. T.; Shaegh, S. A. M., *Fundamentals and applications of microfluidics*. Artech house: 2019.
48. Aulton, M. E., *Pharmaceutics: The science of dosage form design*. Churchill livingstone: 2002.
49. Edward, J. T., Molecular volumes and the Stokes-Einstein equation. *Journal of Chemical Education* **1970,** *47* (4), 261.
50. Einstein, A., *Investigations on the Theory of the Brownian Movement*. Courier Corporation: 1956.
51. Zhang, Z.; Zhao, P.; Xiao, G.; Lin, M.; Cao, X., Focusing-enhanced mixing in microfluidic channels. *Biomicrofluidics* **2008,** *2* (1), 14101.
52. Chen, Z.; Bown, M.; O'Sullivan, B.; MacInnes, J.; Allen, R.; Mulder, M.; Blom, M.; van't Oever, R., Performance analysis of a folding flow micromixer. *Microfluidics and Nanofluidics* **2009,** *6* (6), 763-774.

53. Johnson, B. K.; Prud'homme, R. K., Mechanism for rapid self-assembly of block copolymer nanoparticles. *Phys Rev Lett* **2003,** *91* (11), 118302.
54. Chen, T.; Hynninen, A.-P.; Prud'homme, R. K.; Kevrekidis, I. G.; Panagiotopoulos, A. Z., Coarse-grained simulations of rapid assembly kinetics for polystyrene-b-poly (ethylene oxide) copolymers in aqueous solutions. *The Journal of Physical Chemistry B* **2008,** *112* (51), 16357-16366.
55. Ma, J.; Lee, S. M.-Y.; Yi, C.; Li, C.-W., Controllable synthesis of functional nanoparticles by microfluidic platforms for biomedical applications–a review. *Lab on a Chip* **2017,** *17* (2), 209-226.
56. Jahn, A.; Vreeland, W. N.; Gaitan, M.; Locascio, L. E., Controlled Vesicle Self-Assembly in Microfluidic Channels with Hydrodynamic Focusing. *Journal of the American Chemical Society* **2004,** *126* (9), 2674-2675.
57. Jahn, A.; Stavis, S. M.; Hong, J. S.; Vreeland, W. N.; DeVoe, D. L.; Gaitan, M., Microfluidic Mixing and the Formation of Nanoscale Lipid Vesicles. *ACS Nano* **2010,** *4* (4), 2077-2087.
58. Zhao, C.-X.; He, L.; Qiao, S. Z.; Middelberg, A. P. J., Nanoparticle synthesis in microreactors. *Chemical Engineering Science* **2011,** *66* (7), 1463-1479.
59. Therriault, D.; White, S. R.; Lewis, J. A., Chaotic mixing in three-dimensional microvascular networks fabricated by direct-write assembly. *Nature materials* **2003,** *2* (4), 265-271.
60. Kim, S. C.; Sukovich, D. J.; Abate, A. R., Patterning microfluidic device wettability with spatially-controlled plasma oxidation. *Lab on a Chip* **2015,** *15* (15), 3163-3169.
61. Liu, D.; Zhang, H.; Fontana, F.; Hirvonen, J. T.; Santos, H. A., Current developments and applications of microfluidic technology toward clinical translation of nanomedicines. *Advanced drug delivery reviews* **2018,** *128*, 54-83.
62. Falk, L.; Commenge, J. M., Performance comparison of micromixers. *Chemical Engineering Science* **2010,** *65* (1), 405-411.
63. Schikarski, T.; Trzenschiok, H.; Peukert, W.; Avila, M., Inflow boundary conditions determine T-mixer efficiency. *Reaction Chemistry & Engineering* **2019,** *4* (3), 559-568.
64. Schikarski, T.; Trzenschiok, H.; Avila, M.; Peukert, W., Influence of Mixing on the Precipitation of Organic Nanoparticles: A Lagrangian Perspective on Scale‐up Based on Self‐Similar Distributions. *Chemical Engineering & Technology* **2019,** *42* (8), 1635-1642.
65. Günther, A.; Jhunjhunwala, M.; Thalmann, M.; Schmidt, M. A.; Jensen, K. F., Micromixing of Miscible Liquids in Segmented Gas−Liquid Flow. *Langmuir* **2005,** *21* (4), 1547-1555.
66. Günther, A.; Khan, S. A.; Thalmann, M.; Trachsel, F.; Jensen, K. F., Transport and reaction in microscale segmented gas–liquid flow. *Lab on a Chip* **2004,** *4* (4), 278-286.
67. Mazzitelli, S.; Capretto, L.; Quinci, F.; Piva, R.; Nastruzzi, C., Preparation of cell-encapsulation devices in confined microenvironment. *Advanced Drug Delivery Reviews* **2013,** *65* (11), 1533-1555.
68. Ota, S.; Yoshizawa, S.; Takeuchi, S., Microfluidic formation of monodisperse, cell‐sized, and unilamellar vesicles. *Angewandte Chemie International Edition* **2009,** *48* (35), 6533-6537.
69. Lo, C. T.; Jahn, A.; Locascio, L. E.; Vreeland, W. N., Controlled self-assembly of monodisperse niosomes by microfluidic hydrodynamic focusing. *Langmuir* **2010,** *26* (11), 8559-8566.
70. Yaghmur, A.; Ghazal, A.; Ghazal, R.; Dimaki, M.; Svendsen, W. E., A hydrodynamic flow focusing microfluidic device for the continuous production of hexosomes based on docosahexaenoic acid monoglyceride. *Physical Chemistry Chemical Physics* **2019,** *21* (24), 13005-13013.
71. Capretto, L.; Mazzitelli, S.; Brognara, E.; Lampronti, I.; Carugo, D.; Hill, M.; Zhang, X.; Gambari, R.; Nastruzzi, C., Mithramycin encapsulated in polymeric micelles by microfluidic technology as novel therapeutic protocol for beta-thalassemia. *International journal of nanomedicine* **2012,** *7*, 307-324.
72. Hood, R. R.; DeVoe, D. L.; Atencia, J.; Vreeland, W. N.; Omiatek, D. M., A facile route to the synthesis of monodisperse nanoscale liposomes using 3D microfluidic hydrodynamic focusing in a concentric capillary array. *Lab on a Chip* **2014,** *14* (14), 2403-2409.
73. Liu, Y.; Cheng, C.; Prud'homme, R. K.; Fox, R. O., Mixing in a multi-inlet vortex mixer (MIVM) for flash nano-precipitation. *Chemical Engineering Science* **2008,** *63* (11), 2829-2842.

74. Chow, S. F.; Sun, C. C.; Chow, A. H. L., Assessment of the relative performance of a confined impinging jets mixer and a multi-inlet vortex mixer for curcumin nanoparticle production. *European Journal of Pharmaceutics and Biopharmaceutics* **2014,** *88* (2), 462-471.
75. Liu, R. H.; Stremler, M. A.; Sharp, K. V.; Olsen, M. G.; Santiago, J. G.; Adrian, R. J.; Aref, H.; Beebe, D. J., Passive mixing in a three-dimensional serpentine microchannel. *Journal of microelectromechanical systems* **2000,** *9* (2), 190-197.
76. Hessel, V.; Hardt, S.; Löwe, H.; Schönfeld, F., Laminar mixing in different interdigital micromixers: I. Experimental characterization. *AIChE Journal* **2003,** *49* (3), 566-577.
77. He, B.; Burke, B. J.; Zhang, X.; Zhang, R.; Regnier, F. E., A picoliter-volume mixer for microfluidic analytical systems. *Analytical Chemistry* **2001,** *73* (9), 1942-1947.
78. Stroock, A. D.; Dertinger, S. K.; Ajdari, A.; Mezic, I.; Stone, H. A.; Whitesides, G. M., Chaotic mixer for microchannels. *Science* **2002,** *295* (5555), 647-51.
79. Webb, C.; Forbes, N.; Roces, C. B.; Anderluzzi, G.; Lou, G.; Abraham, S.; Ingalls, L.; Marshall, K.; Leaver, T. J.; Watts, J. A.; Aylott, J. W.; Perrie, Y., Using microfluidics for scalable manufacturing of nanomedicines from bench to GMP: A case study using protein-loaded liposomes. *International Journal of Pharmaceutics* **2020,** *582*, 119266.
80. Li, J.; Xia, G.; Li, Y., Numerical and experimental analyses of planar asymmetric split-and-recombine micromixer with dislocation sub-channels. *Journal of Chemical Technology & Biotechnology* **2013,** *88* (9), 1757-1765.
81. Lee, C.-Y.; Wang, W.-T.; Liu, C.-C.; Fu, L.-M., Passive mixers in microfluidic systems: A review. *Chemical Engineering Journal* **2016,** *288*, 146-160.
82. Xu, Z.; Lu, C.; Riordon, J.; Sinton, D.; Moffitt, M. G., Microfluidic Manufacturing of Polymeric Nanoparticles: Comparing Flow Control of Multiscale Structure in Single-Phase Staggered Herringbone and Two-Phase Reactors. *Langmuir* **2016,** *32* (48), 12781-12789.
83. Thiermann, R.; Mueller, W.; Montesinos-Castellanos, A.; Metzke, D.; Löb, P.; Hessel, V.; Maskos, M., Size controlled polymersomes by continuous self-assembly in micromixers. *Polymer* **2012,** *53* (11), 2205-2210.
84. Kimura, N.; Maeki, M.; Sato, Y.; Note, Y.; Ishida, A.; Tani, H.; Harashima, H.; Tokeshi, M., Development of the iLiNP Device: Fine Tuning the Lipid Nanoparticle Size within 10 nm for Drug Delivery. *ACS Omega* **2018,** *3* (5), 5044-5051.
85. Lim, J.-M.; Swami, A.; Gilson, L. M.; Chopra, S.; Choi, S.; Wu, J.; Langer, R.; Karnik, R.; Farokhzad, O. C., Ultra-high throughput synthesis of nanoparticles with homogeneous size distribution using a coaxial turbulent jet mixer. *ACS nano* **2014,** *8* (6), 6056-6065.
86. He, Y.; Park, K., Effects of the Microparticle Shape on Cellular Uptake. *Molecular Pharmaceutics* **2016,** *13* (7), 2164-2171.
87. Hao, N.; Nie, Y.; Zhang, J. X. J., Microfluidic Flow Synthesis of Functional Mesoporous Silica Nanofibers with Tunable Aspect Ratios. *ACS Sustainable Chemistry & Engineering* **2018,** *6* (2), 1522-1526.
88. Dashtimoghadam, E.; Mirzadeh, H.; Taromi, F. A.; Nyström, B., Microfluidic self-assembly of polymeric nanoparticles with tunable compactness for controlled drug delivery. *Polymer* **2013,** *54* (18), 4972-4979.
89. Liu, D.; Bernuz, C. R.; Fan, J.; Li, W.; Correia, A.; Hirvonen, J.; Santos, H. A., A Nano-in-Nano Vector: Merging the Best of Polymeric Nanoparticles and Drug Nanocrystals. *Advanced Functional Materials* **2017,** *27* (9), 1604508.
90. Sun, J.; Zhang, L.; Wang, J.; Feng, Q.; Liu, D.; Yin, Q.; Xu, D.; Wei, Y.; Ding, B.; Shi, X.; Jiang, X., Tunable Rigidity of (Polymeric Core)–(Lipid Shell) Nanoparticles for Regulated Cellular Uptake. *Advanced Materials* **2015,** *27* (8), 1402-1407.
91. Lee, T. Y.; Choi, T. M.; Shim, T. S.; Frijns, R. A. M.; Kim, S.-H., Microfluidic production of multiple emulsions and functional microcapsules. *Lab on a Chip* **2016,** *16* (18), 3415-3440.
92. Sapei, L.; Naqvi, M. A.; Rousseau, D., Stability and release properties of double emulsions for food applications. *Food Hydrocolloids* **2012,** *27* (2), 316-323.

93. Duncanson, W. J.; Lin, T.; Abate, A. R.; Seiffert, S.; Shah, R. K.; Weitz, D. A., Microfluidic synthesis of advanced microparticles for encapsulation and controlled release. *Lab on a Chip* **2012,** *12* (12), 2135-2145.
94. Jo, Y. K.; Lee, D., Biopolymer Microparticles Prepared by Microfluidics for Biomedical Applications. *Small* **2020,** *16* (9), 1903736.
95. Michelon, M.; Huang, Y.; de la Torre, L. G.; Weitz, D. A.; Cunha, R. L., Single-step microfluidic production of W/O/W double emulsions as templates for β-carotene-loaded giant liposomes formation. *Chemical Engineering Journal* **2019,** *366*, 27-32.
96. Jeong, W.-C.; Choi, M.; Lim, C. H.; Yang, S.-M., Microfluidic synthesis of atto-liter scale double emulsions toward ultrafine hollow silica spheres with hierarchical pore networks. *Lab on a Chip* **2012,** *12* (24), 5262-5271.
97. Moros, M.; Mitchell, S. G.; Fuente, V. G. a. J. M. d. l., The Fate of Nanocarriers As Nanomedicines In Vivo: Important Considerations and Biological Barriers to Overcome. *Current Medicinal Chemistry* **2013,** *20* (22), 2759-2778.
98. Wang, W., Advanced protein formulations. *Protein science : a publication of the Protein Society* **2015,** *24* (7), 1031-1039.
99. Hardin, J. O.; Fernandez-Nieves, A.; Martinez, C. J.; Milam, V. T., Altering colloidal surface functionalization using DNA encapsulated inside monodisperse gelatin microsphere templates. *Langmuir : the ACS journal of surfaces and colloids* **2013,** *29* (18), 5534-5539.
100. Solomun, J. I.; Totten, J. D.; Wongpinyochit, T.; Florence, A. J.; Seib, F. P., Manual Versus Microfluidic-Assisted Nanoparticle Manufacture: Impact of Silk Fibroin Stock on Nanoparticle Characteristics. *ACS Biomaterials Science & Engineering* **2020,** *6* (5), 2796-2804.
101. Grimaldi, N.; Andrade, F.; Segovia, N.; Ferrer-Tasies, L.; Sala, S.; Veciana, J.; Ventosa, N., Lipid-based nanovesicles for nanomedicine. *Chem Soc Rev* **2016,** *45* (23), 6520-6545.
102. Wang, H.; Jiang, Y.; Peng, H.; Chen, Y.; Zhu, P.; Huang, Y., Recent progress in microRNA delivery for cancer therapy by non-viral synthetic vectors. *Advanced Drug Delivery Reviews* **2015,** *81*, 142-160.
103. Cheng, X.; Lee, R. J., The role of helper lipids in lipid nanoparticles (LNPs) designed for oligonucleotide delivery. *Advanced Drug Delivery Reviews* **2016,** *99*, 129-137.
104. Suk, J. S.; Xu, Q.; Kim, N.; Hanes, J.; Ensign, L. M., PEGylation as a strategy for improving nanoparticle-based drug and gene delivery. *Advanced Drug Delivery Reviews* **2016,** *99*, 28-51.
105. Wang, Y.; Miao, L.; Satterlee, A.; Huang, L., Delivery of oligonucleotides with lipid nanoparticles. *Advanced Drug Delivery Reviews* **2015,** *87*, 68-80.
106. Dawidczyk, C. M.; Kim, C.; Park, J. H.; Russell, L. M.; Lee, K. H.; Pomper, M. G.; Searson, P. C., State-of-the-art in design rules for drug delivery platforms: Lessons learned from FDA-approved nanomedicines. *Journal of Controlled Release* **2014,** *187*, 133-144.
107. Kamiya, K.; Kawano, R.; Osaki, T.; Akiyoshi, K.; Takeuchi, S., Cell-sized asymmetric lipid vesicles facilitate the investigation of asymmetric membranes. *Nat Chem* **2016,** *8* (9), 881-9.
108. Mizuno, M.; Toyota, T.; Konishi, M.; Kageyama, Y.; Yamada, M.; Seki, M., Formation of monodisperse hierarchical lipid particles utilizing microfluidic droplets in a nonequilibrium state. *Langmuir : the ACS journal of surfaces and colloids* **2015,** *31* (8), 2334-2341.
109. Kitazoe, K.; Wang, J.; Kaji, N.; Okamoto, Y.; Tokeshi, M.; Kogure, K.; Harashima, H.; Baba, Y., A touch-and-go lipid wrapping technique in microfluidic channels for rapid fabrication of multifunctional envelope-type gene delivery nanodevices. *Lab on a Chip* **2011,** *11* (19), 3256-3262.
110. Nakamura, T.; Kawai, M.; Sato, Y.; Maeki, M.; Tokeshi, M.; Harashima, H., The Effect of Size and Charge of Lipid Nanoparticles Prepared by Microfluidic Mixing on Their Lymph Node Transitivity and Distribution. *Mol Pharm* **2020,** *17* (3), 944-953.
111. Zhang, H.; Tumarkin, E.; Sullan, R. M. A.; Walker, G. C.; Kumacheva, E., Exploring Microfluidic Routes to Microgels of Biological Polymers. *Macromolecular Rapid Communications* **2007,** *28* (5), 527-538.
112. Gunduz, O.; Ahmad, Z.; Stride, E.; Edirisinghe, M., Continuous generation of ethyl cellulose drug delivery nanocarriers from microbubbles. *Pharm Res* **2013,** *30* (1), 225-37.

113. Valencia, P. M.; Pridgen, E. M.; Rhee, M.; Langer, R.; Farokhzad, O. C.; Karnik, R., Microfluidic Platform for Combinatorial Synthesis and Optimization of Targeted Nanoparticles for Cancer Therapy. *ACS Nano* **2013,** *7* (12), 10671-10680.
114. Chronopoulou, L.; Sparago, C.; Palocci, C., A modular microfluidic platform for the synthesis of biopolymeric nanoparticles entrapping organic actives. *Journal of nanoparticle research* **2014,** *16* (11), 2703.
115. Hu, Y.; Wang, Q.; Wang, J.; Zhu, J.; Wang, H.; Yang, Y., Shape controllable microgel particles prepared by microfluidic combining external ionic crosslinking. *Biomicrofluidics* **2012,** *6* (2), 026502.
116. Koh, C. G.; Kang, X.; Xie, Y.; Fei, Z.; Guan, J.; Yu, B.; Zhang, X.; Lee, L. J., Delivery of Polyethylenimine/DNA Complexes Assembled in a Microfluidics Device. *Molecular Pharmaceutics* **2009,** *6* (5), 1333-1342.
117. Capretto, L.; Cheng, W.; Carugo, D.; Katsamenis, O. L.; Hill, M.; Zhang, X., Mechanism of co-nanoprecipitation of organic actives and block copolymers in a microfluidic environment. *Nanotechnology* **2012,** *23* (37), 375602.
118. Xie, H.; She, Z.-G.; Wang, S.; Sharma, G.; Smith, J. W., One-Step Fabrication of Polymeric Janus Nanoparticles for Drug Delivery. *Langmuir* **2012,** *28* (9), 4459-4463.
119. Hong, S. H.; Patel, T.; Ip, S.; Garg, S.; Oh, J. K., Microfluidic Assembly To Synthesize Dual Enzyme/Oxidation-Responsive Polyester-Based Nanoparticulates with Controlled Sizes for Drug Delivery. *Langmuir* **2018,** *34* (10), 3316-3325.
120. Wang, J.-X.; Zhang, Q.-X.; Zhou, Y.; Shao, L.; Chen, J.-F., Microfluidic synthesis of amorphous cefuroxime axetil nanoparticles with size-dependent and enhanced dissolution rate. *Chemical Engineering Journal* **2010,** *162* (2), 844-851.
121. Zhao, H.; Wang, J.-X.; Wang, Q.-A.; Chen, J.-F.; Yun, J., Controlled Liquid Antisolvent Precipitation of Hydrophobic Pharmaceutical Nanoparticles in a Microchannel Reactor. *Industrial & Engineering Chemistry Research* **2007,** *46* (24), 8229-8235.
122. Liu, K.; Zhu, Z.; Wang, X.; Gonçalves, D.; Zhang, B.; Hierlemann, A.; Hunziker, P., Microfluidics-based single-step preparation of injection-ready polymeric nanosystems for medical imaging and drug delivery. *Nanoscale* **2015,** *7* (40), 16983-16993.
123. Li, W.; Liu, D.; Zhang, H.; Correia, A.; Mäkilä, E.; Salonen, J.; Hirvonen, J.; Santos, H. A., Microfluidic assembly of a nano-in-micro dual drug delivery platform composed of halloysite nanotubes and a pH-responsive polymer for colon cancer therapy. *Acta Biomaterialia* **2017,** *48*, 238-246.
124. He, J.; Wei, Z.; Wang, L.; Tomova, Z.; Babu, T.; Wang, C.; Han, X.; Fourkas, J. T.; Nie, Z., Hydrodynamically Driven Self‐Assembly of Giant Vesicles of Metal Nanoparticles for Remote‐Controlled Release. *Angewandte Chemie* **2013,** *125* (9), 2523-2528.
125. Lin, Y.-S.; Yang, C.-H.; Hsu, Y.-Y.; Hsieh, C.-L., Microfluidic synthesis of tail-shaped alginate microparticles using slow sedimentation. *ELECTROPHORESIS* **2013,** *34* (3), 425-431.
126. Chen, S.; Tam, Y. Y. C.; Lin, P. J. C.; Sung, M. M. H.; Tam, Y. K.; Cullis, P. R., Influence of particle size on the in vivo potency of lipid nanoparticle formulations of siRNA. *Journal of Controlled Release* **2016,** *235*, 236-244.
127. Lou, G.; Anderluzzi, G.; Woods, S.; Roberts, C. W.; Perrie, Y., A novel microfluidic-based approach to formulate size-tuneable large unilamellar cationic liposomes: Formulation, cellular uptake and biodistribution investigations. *European Journal of Pharmaceutics and Biopharmaceutics* **2019,** *143*, 51-60.
128. Shallan, A. I.; Priest, C., Microfluidic process intensification for synthesis and formulation in the pharmaceutical industry. *Chemical Engineering and Processing - Process Intensification* **2019,** *142*, 107559.
129. Jensen, K. F., Flow chemistry—Microreaction technology comes of age. *AIChE Journal* **2017,** *63* (3), 858-869.
130. Chang, C.-H.; Paul, B. K.; Remcho, V. T.; Atre, S.; Hutchison, J. E., Synthesis and post-processing of nanomaterials using microreaction technology. *Journal of Nanoparticle Research* **2008,** *10* (6), 965-980.

131. Amador, C.; Gavriilidis, A.; Angeli, P., Flow distribution in different microreactor scale-out geometries and the effect of manufacturing tolerances and channel blockage. *Chemical Engineering Journal* **2004,** *101* (1-3), 379-390.
132. Ying, Y.; Chen, G.; Zhao, Y.; Li, S.; Yuan, Q., A high throughput methodology for continuous preparation of monodispersed nanocrystals in microfluidic reactors. *Chemical Engineering Journal* **2008,** *135* (3), 209-215.
133. Valdeperez, D.; Wang, T.; Eußner, J. P.; Weinert, B.; Hao, J.; Parak, W. J.; Dehnen, S.; Pelaz, B., Polymer-coated nanoparticles: Carrier platforms for hydrophobic water- and air-sensitive metallo-organic compounds. *Pharmacological Research* **2017,** *117*, 261-266.
134. Lin, C.-A. J.; Sperling, R. A.; Li, J. K.; Yang, T.-Y.; Li, P.-Y.; Zanella, M.; Chang, W. H.; Parak, W. J., Design of an Amphiphilic Polymer for Nanoparticle Coating and Functionalization. *Small* **2008,** *4* (3), 334-341.
135. Song, W.; Su, X.; Gregory, D. A.; Li, W.; Cai, Z.; Zhao, X., Magnetic Alginate/Chitosan Nanoparticles for Targeted Delivery of Curcumin into Human Breast Cancer Cells. *Nanomaterials* **2018,** *8* (11), 907.
136. Chastek, T. Q.; Iida, K.; Amis, E. J.; Fasolka, M. J.; Beers, K. L., A microfluidic platform for integrated synthesis and dynamic light scattering measurement of block copolymer micelles. *Lab on a Chip* **2008,** *8* (6), 950-957.
137. Dootz, R.; Otten, A.; Köster, S.; Struth, B.; Pfohl, T., Evolution of DNA compaction in microchannels. *Journal of Physics: Condensed Matter* **2006,** *18* (18), S639.
138. Ho, Y.-P.; Chen, H. H.; Leong, K. W.; Wang, T.-H., The convergence of quantum-dot-mediated fluorescence resonance energy transfer and microfluidics for monitoring DNA polyplex self-assembly in real time. *Nanotechnology* **2009,** *20* (9), 095103.